Experiments in Fluids 14, 423–432 (1993)

Experiments in Fluids

An experimental study of two flows through an axisymmetric sudden expansion

W. J. Devenport, E. P. Sutton

Cambridge University Engineering Department, Trumpington Street, Cambridge, Great Britain

Received: 25 February 1992/Accepted: 18 September 1992

Abstract. Two turbulent separated and reattaching flows produced by a sudden expansion in a pipe have been studied. The first was produced by a simple axisymmetric sudden enlargement from a nozzle of diameter 80 mm to a pipe of diameter 150 mm. The second was the flow at the same enlargement with the addition of a centerbody 90 mm downstream of the nozzle exit. Detailed measurements of velocity and skin friction (made primarily using pulsed wires) and of wall static pressure are presented. Without the centerbody the flow structure is similar to that observed in other sudden pipe expansions and over backward-facing steps. A turbulent free shear layer, bearing some similarity to that of a round jet, grows from separation and then reattaches to the pipe wall downstream. Reattachment is a comparatively gradual process, the shear layer approaching the wall at a glancing angle. The introduction of the centerbody causes the shear layer to curve towards the wall and reattach at a much steeper angle. Reattachment is much more rapid; gradients of skin friction and pressure along the wall are many times those without the centerbody. The high curvature of the shear layer strongly influences its turbulent structure, locally suppressing turbulence levels and reducing its growth rate.

1 Introduction

The basic features of high Reynolds number flow through a sudden expansion are well known (Fig. 1). The oncoming flow separates at the expansion forming a turbulent free shear layer. The shear layer grows by entraining fluid from the main stream and from a region of recirculation formed adjacent to the wall. Pressure in the recirculation region is on the whole slightly lower than in the main stream and thus the shear layer curves towards the wall. In the resulting reattachment region some fluid from the shear layer is passed upstream into the region of recirculating flow, replacing that originally entrained. Recovery of the flow downstream of reattachment is slow; the influence of the wall propagating only slowly through the shear layer.

There have been numerous experimental investigations of this type of flow. The majority have concentrated on the two-dimensional backward-facing step. Table 1 summarizes some of these investigations. Perhaps most well known are

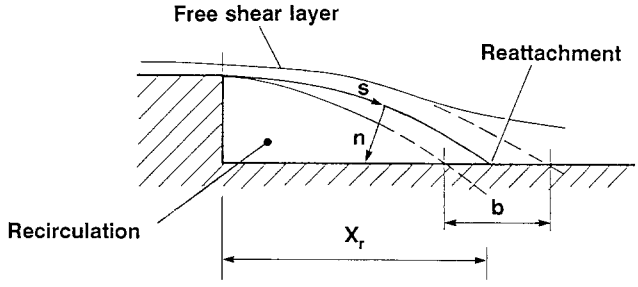

Fig. 1. Major features of flow through a sudden expansion

those by Eaton and Johnston (1980) and others at Stanford University and NASA Ames. Apart from documenting the structure these studies also examined effects of boundary-layer thickness and state at separation, expansion ratio and mild adverse pressure gradient. Eaton and Johnson (1980), in particular, stressed the importance of the distance from separation to reattachment, X_r (termed "reattachment length") as a scaling parameter in this type flow. Use of this parameter dates back to the work of Roshko and Lau (1965) who showed that, with streamwise distance normalized on X_r, wall static pressure distributions measured on the reattachment surface over a range of conditions and geometries collapse to a single curve. The reattachment length for high-Reynolds number backstep flows usually lies between about 6 and 8 step heights, see Table 1.

Considerably less has been done on axisymmetric sudden expansions, although this is arguably a more practically relevant configuration. Table 1 summarizes some investigations. Studies in which velocities were not measured (for example Runchal 1971, Baughn et al. 1984) and studies in which the sudden expansion was followed by a contraction, as in a combustor (for example, Drewry 1978, Yang and Yu 1983) are excluded from this table. Most notable in Table 1 is the work done by Durrett et al. (1988), Gould et al. (1990) and Stevenson et al. (1984) who used LDV to measure mean velocities and turbulence quantities in several axisymmetric configurations.

Correspondence to: W. J. Devenport

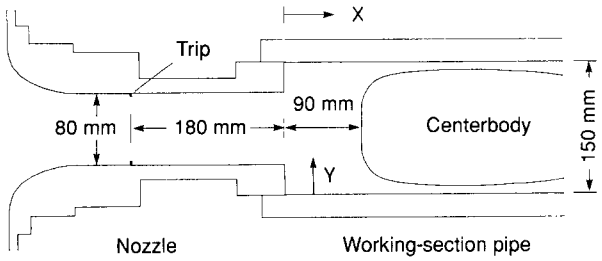

Fig. 2. Cross section of the nozzle and working-section pipe

Table 1. Some investigations of two-dimensional and axisymmetric sudden expansion flows summarized in terms of expansion ratio (E.R.), Reynolds number based on step height H and potential-flow velocity at separation (Re_H), boundary layer thickness δ and distance to reattachment X_r.

Author	E.R.	$Re_H \cdot 10^{-4}$	δ/H	X_r/H
Backward-facing step				
Adams et al. (1984)	1.25	3.6	1.00	6.36
Cherry et al. (1984)	1.04	1.5	0.3?	6.86
Driver and Seegmuller (1985)	1.13	3.6	1.50	6.10
Eaton and Johnston (1980)	1.67	3.8	0.20	7.95
Kim et al. (1978)	1.50	4.5	0.30	7?
Moss and Baker (1980)	1.10	5.0	0.70	5.91
Pronchick and Kline (1983)	1.42	1.4	0.66	6.50
Westphal et al. (1984)	1.67	4.2	0.36	8.55
Axisymmetric expansion				
Durrett et al. (1988)	3.61	8.4	?	8.4
Freeman (1975)	4.41	1.6	0.91	8.8
Gould et al. (1990)	4.0	5.6	0.16	~8
Ha Minh and Chassaing (1979)	4.0	7.2	0.30	>8.6
Khezzar et al. (1985)	3.06	1.5	0.45	9.3
Moon and Rudinger (1977)	2.04	0.6	?	8.5
Stevenson et al. (1984)	3.51	3.6	?	>8
Present datum flow	3.52	3.5	0.21	10.7

The purpose of this paper is to present an experimental study of two axisymmetric flows. The first, which we shall refer to as the datum flow, was produced by a simple axisymmetric sudden enlargement (similar to those of Table 1) from a nozzle of diameter 80 mm to a pipe of diameter 150 mm (Fig. 2). The second was the flow at the same enlargement with the addition of a centerbody 90 mm downstream of the nozzle exit. The shape of the centerbody was computed using a potential-flow method to give an approximation to a specified pressure distribution (see Devenport 1985). The maximum diameter of the centerbody was 132.7 mm, making the cross-sectional area of the annulus between the centerbody and pipe approximately three quarters of that of the pipe.

The application driving this work was those separated flows formed behind the slat and in the flap cove of multi-element airfoils. These flows reattach in regions where the streamlines of the outer flow are converging. The centerbody was intended to reproduce this convergence.

2 Apparatus and instrumentation

The nozzle and sudden expansion shown in Fig. 2 formed part of a small axisymmetric wind tunnel. The wind tunnel supplied air to the nozzle from a centrifugal blower through a silencer, wide-angle diffuser with screens, a settling chamber and a honeycomb, and finally a 126:1 contraction, the latter part of which is visible in Fig. 2. Boundary-layer bleed was used to prevent the formation and amplification of streamwise vorticity on the walls of the contraction. Flow conditions at the nozzle exit were essentially the same in both cases. The flow here consisted of a closely uniform potential core, with a mean velocity U_{ref} of 15 m/s and an axial turbulence intensity of 0.4%, surrounded by an axisymmetric boundary layer. The boundary layer was turbulent having been tripped 180 mm upstream. It was approximately 7 mm thick and had a momentum thickness Reynolds number of 660. Its mean velocity and turbulence intensity profiles closely resembled those of a two-dimensional equilibrium boundary layer of the same Reynolds number.

Based on U_{ref} and the step height H (of 35 mm) the Reynolds number was 35,000. Mean surface pressure measurements made on the pipe wall showed both flows to be closely axisymmetric and showed little change in either flow with increase in Reynolds number (Devenport 1985). Spectra of surface pressure fluctuations measured close to the nozzle exit showed no peaks associated with the blade-passing frequency of the blower. Some peaks associated with resonances in the nozzle and pipe were present but overall noise levels were far too low to have significantly influenced either flow (Devenport 1985).

Pressure, velocity and skin-friction measurements were made in both flows. Mean pressures were measured using taps installed in the wall of the 150 mm pipe. Most velocity and skin friction measurements were made using pulsed-wire anemometry. Pulsed wires sense the time of flight of a heated tracer of air between a pulsing wire and one of two sensor wires. Three different types of probe were used. All were operated using a PELA Flow Instruments Ltd. anemometer unit interfaced to a Commodore CBM 4032 (PET) computer. The operating principles of this unit are described by Bradbury and Castro (1971). A PELA pulsed-wire probe of standard design (as described by Bradbury and Castro (1971)) and a new wall-mounted pulsed wire probe built especially for this investigation (described in detail by Devenport et al. (1990)) were used to measure the axial components of mean velocity and turbulence intensity. Mean and fluctuating skin friction at the pipe wall were measured using a pulsed-wire probe of the type described by Castro et al. (1987). This probe senses velocity in the sublayer, 0.05 mm from the wall, which is assumed proportional to skin friction. Additional velocity measurements outside regions of separated flow were made with hot-wire anemometers. Dantec single and X-array probes, types 55P11, 14, 61 and 64, operated using Prosser type 6110 anemometer bridges interfaced to the PET computer, were used. Where necessary hot-wire mea-

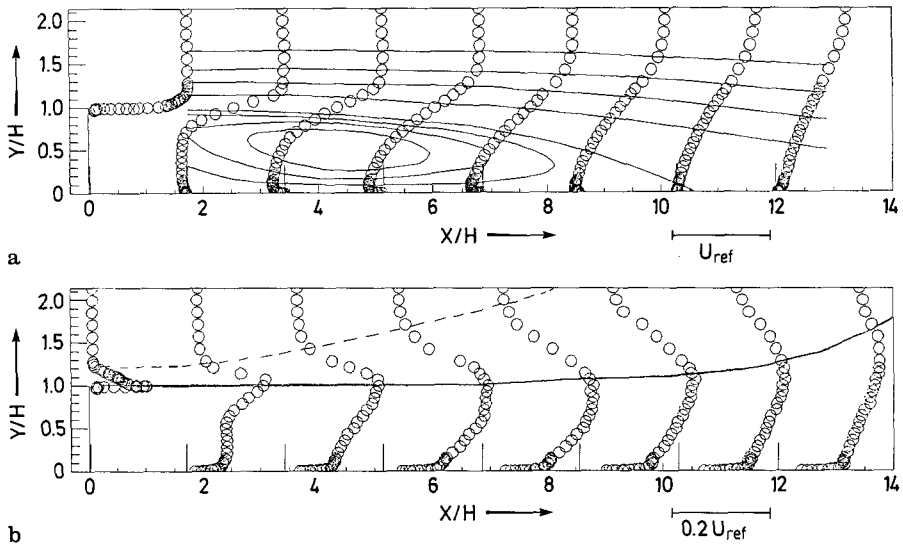

Fig. 3a and b. Velocity measurements in the datum flow. **a** Profiles of mean axial velocity U/U_{ref} and streamlines deduced from them; **b** profiles of axial turbulence intensity u'/U_{ref}, locus of peak streamwise turbulence intensity (solid line) and, locus of 0.99 stagnation pressure coefficient (dashed line). Note distorted axial scale

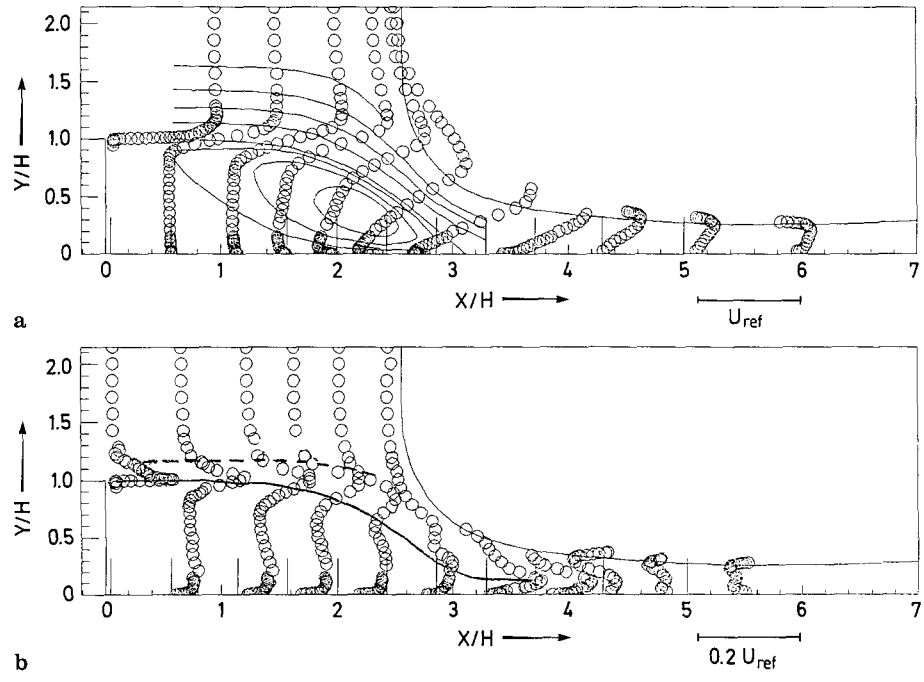

Fig. 4a and b. Velocity measurements in the flow with centerbody. **a** Profiles of mean axial velocity U/U_{ref} and streamlines deduced from them; **b** profiles of axial turbulence intensity u'/U_{ref}, locus of peak streamwise turbulence intensity (solid line) and, locus of 0.99 stagnation pressure coefficient (dashed line)

surements were corrected for the effects of high local turbulence levels using the methods of Tutu and Chevray (1975) and Yavuzkurt (1984).

All probes were introduced to the flow through ports in the wall of the pipe. Velocity probes were calibrated frequently in the potential core at the nozzle exit. The velocity here was known from pressure measurements and could be varied by altering the blower speed. The pulsed-wire skin friction meter was calibrated for wall shear stress against a Preston tube. Both were placed under an equilibrium turbulent boundary layer whose edge velocity could be varied.

Uncertainties in measurements, calculated using the method of Kline and McClintock (1953), are listed in Table 2.

3 Results

Measurements are presented using the coordinate system (X,Y) defined in Fig. 2; X being measured axially downstream from the step and Y radially inward from the pipe wall. Figures 3a and 4a show profiles of mean axial velocity U/U_{ref} and time averaged streamlines deduced from them. Variations in the total mass flux indicated by the profiles were less than $\pm 2\%$ in both flows, consistent with the axisymmetry of the flows and the uncertainty in U. Figures 3b and 4b show profiles of axial turbulence intensity u'/U_{ref}. Coefficients of mean surface pressure $C_p=(p-p_{ref})/\frac{1}{2}\varrho U_{ref}^2$, mean skin friction $C_f=\tau_w/\frac{1}{2}\varrho U_{ref}^2$ and of the r.m.s. of skin-friction fluctuations $C_{f\,r.m.s.}=\tau'_w/\frac{1}{2}\varrho U_{ref}^2$ measured along the

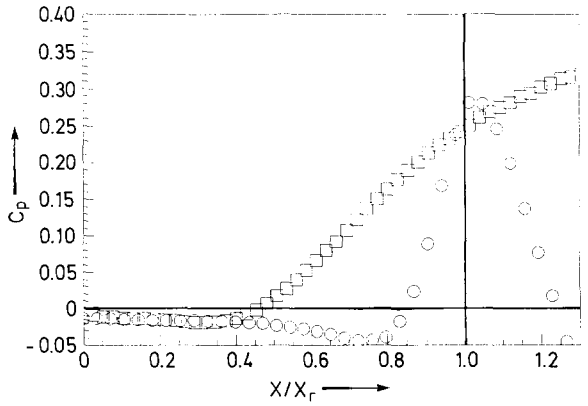

Fig. 5. Distribution of mean surface pressure coefficient along the pipe wall; squares, datum flow; circles, flow with centerbody

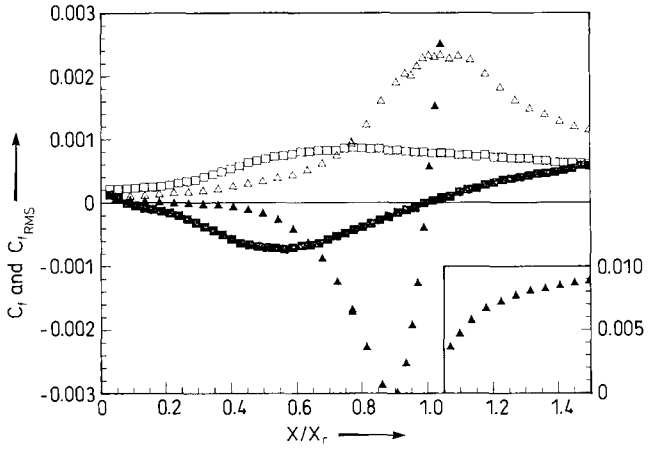

Fig. 6. Skin-friction distributions for the datum flow (squares) and flow with centerbody (triangles); solid symbols, C_f; open symbols $C_{f\,\mathrm{r.m.s.}}$

Table 2. Uncertainty estimates

Quantity	Uncertainty
Mean velocity U/U_{ref}	± 0.02
Turbulence intensity u'/U_{ref}	± 0.01
Pressure coefficient C_p	± 0.004
Skin-friction coefficients	
C_f	$\pm 6\%$
$C_{f\,\mathrm{r.m.s}}$	$\pm 6\%$

pipe wall are plotted in Figs. 5 and 6. Here p_{ref} represents the wall static pressure 10 mm upstream of the nozzle exit, a close approximation to the static pressure at separation.

Reattachment positions were measured using the pulsed-wire skin-friction probe as the point of zero time-average skin friction. In the datum flow the axial distance from separation to reattachment X_r was $(10.7 \pm .28)$ H, circumferential variations in X_r being within the uncertainty of its measurement. In the flow with centerbody X_r was only $(3.15 \pm .08)$ H.

4 Discussion

4.1 Datum flow

4.1.1 Velocity field

The velocity measurements (Fig. 3) clearly show the separation of the flow at the step, the formation of a turbulent shear layer and its reattachment to the wall downstream. The velocity gradient associated with the shear layer, and its relaxation, is clearly visible in the mean-velocity measurements, as is the region of recirculation enclosed by the reattachment process. Time-averaged backflow velocities reach a maximum of 0.16 U_{ref} at $X/X_r = 0.48$.

For a short distance downstream of separation ($X/H < 6$) the potential core, the turbulent mixing layer and the recirculation region are fairly distinct. The development of the mixing layer here may be compared with that of a round jet since the influence of the reattachment surface is felt only indirectly through the presence of the recirculation zone. Husain and Husain (1979) studied a round jet shear layer formed from a turbulent boundary layer. Their jet had a Reynolds number $U_{\mathrm{ref}} d_1/\nu$ of 2.5×10^5 and an initial boundary layer displacement thickness δ_1/d_1 of 8×10^{-3}, where d_1 is the initial jet diameter. This compares with 0.8×10^5 and 12×10^{-3} for the datum flow. The development of these two shear layers is compared in Fig. 7 in terms of the streamwise variation of the peak turbulence intensity u'_p/U_{ref} and of the vorticity thickness $\delta_\omega = U_e / \left.\frac{\partial U}{\partial Y}\right|_{\max}$ where U_e is the local maximum velocity on the high-speed side of the shear layer[1]. Axial mean-velocity profiles of the two layers are compared in Fig. 8 using the coordinate $(Y - Y_{0.5})/\delta_\omega$, where $Y_{0.5}$ is the location where $U = 0.5\,U_e$.

The profiles are all very similar in shape, those of the datum flow falling only slightly below that of the jet towards the low speed side of the layer because of the reversed flow here. The rate of relaxation of the mean-velocity gradient, as indicated by the growth rate of vorticity thickness, $d\delta_w/dX$, is 0.117 in the initial region of the jet mixing layer and becomes 0.175 downstream of $X/d_1 = 1.5$. For the datum flow, however, $d\delta_w/dX$ is much lower at about 0.094 and remains almost constant. Peak turbulence levels (Fig. 7 a) are significantly greater and grow at a faster rate in the reattaching mixing layer, right from separation.

Hussain and Husain (1980) have shown that the development of the jet mixing layer begins as an instability in the separating boundary layer. This then causes the roll up of large-scale predominantly circumferential coherent struc-

[1] Note that in our definition of vorticity thickness we have effectively chosen a velocity of zero for the low speed side of the reattaching shear layer. This choice is necessarily rather arbitrary since the low speed edge of the layer is very poorly defined. An alternative would be to use local peak backflow velocity. However, this is no better since it treats the backflow as though it were a boundary condition of the shear layer and not also a consequence. In addition this choice leads to a poorer collapse of the datum flow velocity profiles in Fig. 8

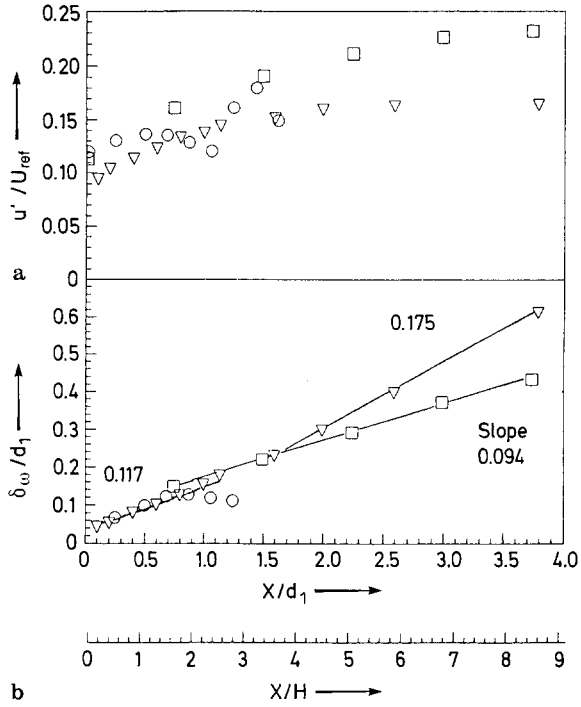

Fig. 7a and b. Comparison of distributions of **a** peak turbulence intensity, and **b** vorticity thickness in the datum flow (squares), flow with centerbody (circles) and the axisymmetric jet of Husain and Hussain (1979) (triangles)

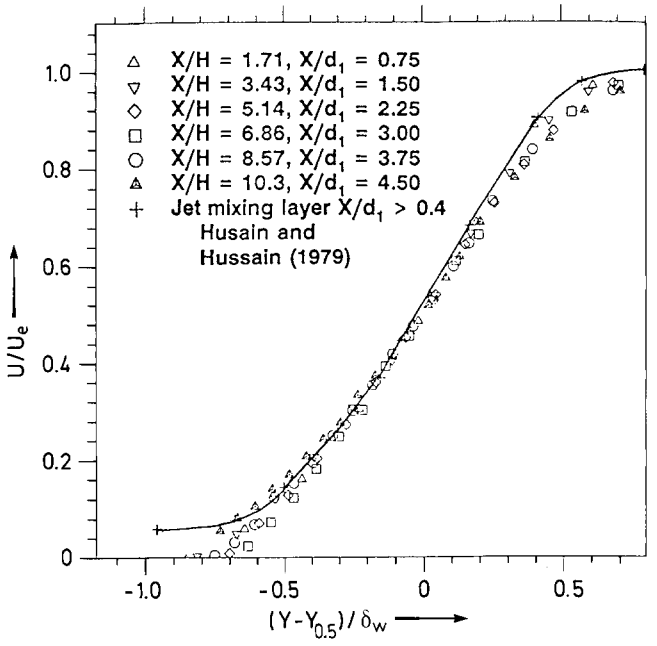

Fig. 8. Comparison of mean velocity profiles in the shear layer of the datum flow and in Husain and Hussain's (1979) axisymmetry jet

tures that grow and pair with distance downstream. Husain and Hussain attribute the change of $d\delta_w/dX$ in their flow to the onset of pairing. The above results suggest that the reattaching shear layer contains turbulent structures that are less efficient at mixing (hence the lower growth rate of δ_ω) and less well organzied (hence the lack of evidence of pairing in the growth rate). This is probably because the structures

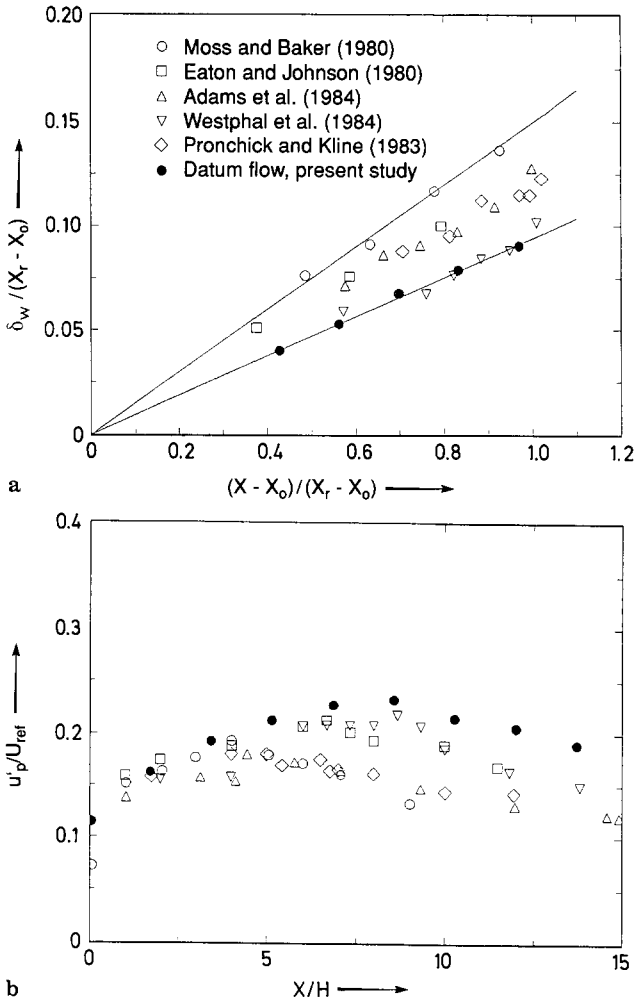

Fig. 9a and b. Comparison of the datum flow and some-two-dimensional flows over backward-facing steps. **a** Vorticity thickness, **b** peak streamwise turbulence intensity

are more three dimensional. Significant three dimensionality in the shear layer structures of two-dimensional backstep flows has been observed by Bandyopadhyay (1991) and others. A slower growing, more three dimensional, shear layer appears at first sight inconsistent with the higher turbulence levels. It may be that these elevated levels are caused by low-frequency "flapping" of the shear layer, as proposed by Eaton and Johnson (1980), or other low-frequency fractures of a more three-dimensional nature. Such motions would not necessarily increase the apparent growth rate of the shear layer unless they increased sufficiency in magnitude with distance downstream. This seems unlikely since they would probably be inhibited as the shear layer approached the reattachment surface.

Figure 9 compares the variations of δ_ω and u'_p/U_{ref} for the datum flow with those from a number of plane two-dimensional flows over backward-facing steps. To make the comparison of δ_ω, the virtual origin of its growth X_0 ($= -2.0$ H in the datum flow) has been subtracted out in each case. The initial development of u'_p/U_{ref} is much the same in the datum

flow as in the two-dimensional flows. $d\delta_w/dX$, on the other hand, appears on the low side. It is worth noting, however, the range of shear layer growth rates for the reattaching flows represented in Fig. 9 a, 0.094 to 0.15. Gutmark and Ho (1983) cite a number of different growth rates for vorticity thickness in axisymmetric and two-dimensional jet shear layers, almost all of which fall between 0.14 and 0.22. This supports our inference that on time average the presence of the recirculation region substantially inhibits the rate of relaxation of the mean-velocity gradient in reattaching shear layers.

Over the downstream half of the separation region ($X/H > 6$, Fig. 3) the clear distinction between the separated shear layer and the recirculation region vanishes, particularly in the turbulence intensity profiles. By $X/H = 8$ the shear layer has engulfed the potential core, defined as the region in which the stagnation-pressure coefficient $C_{p0} = (p_0 - p_{ref})/\frac{1}{2}\varrho U_{ref}^2$ is greater than 0.99. The distance to reattachment, 10.7 H, is large when compared with typical values for plane two-dimensional step flows (Table 1), being more in line with observations made for other sudden pipe expansions. This difference presumably results from the fact that, relative to its surface area available for entrainment, the separated shear layer has to entrain a greater volume of recirculating fluid before reattaching in the axisymmetric than in the two-dimensional case. Upstream of $X/H = 8.6$ the peak turbulence level in the shear layer continues to rise but at a rate that decreases with distance downstream. The maximum of u'_p/U_{ref} (23.3%), recorded at $X/H = 8.57$, is greater than in the plane two-dimensional flows represented in Fig. 9. This may simply reflect the fact that the separated shear layer has further to develop in the axisymmetric case because of the greater distance to reattachment. The reduction in u'_p/U_{ref} downstream of this location is to some extent artificial since it does not appear when u'_p is normalized on the local edge velocity U_e. In terms of U_e (which becomes the centerline velocity downstream of the potential core), u'_p continues to increase, reaching its maximum value well downstream of mean reattachment, near $X/H = 17$.

The continuing increase may be a consequence of a fairly gradual reattachment. The dividing streamline (Fig. 3 a) suggests that the shear layer approaches the reattachment surface at a glancing angle (17°). The locus of u'_p (Fig. 3 b), however, which may equally well be taken as the center of the shear layer, never approaches the wall, moving only towards the centerline as it would in a free jet. In fact, comparisons made by Devenport (1985) show the mean-velocity and turbulence-intensity profiles developing like those of a free jet as far downstream as $X/H = 13.7$.

The knee in the variation of u'_p/U_{ref} (Fig. 9), centered near $X/H = 10$ is also apparent when u'_p is normalized on U_e. This feature has been observed in plane two-dimensional flows over backward-facing steps by Eaton and Johnston (1980) and others. Eaton and Johnston propose that it results from a reduction in turbulence levels caused by stabilizing curvature of the separated shear layer just upstream of reattachment. While curvature may play a part in the evolution of shear layer turbulence in the present flow, it does not appear to be a very likely cause of this feature. The time average streamlines of Fig. 3 are much more strongly curved between $X/H = 4$ and 8 than they are near $X/H = 10$. Another possibility is that turbulence levels are suppressed by the direct influence of the reattachment surface. Bandyopadhyay (1991) has observed the disintegration of large scale shear layer structures as they interact with the wall in the reattachment region of a backstep flow that, presumably, would result in a local reduction in u'_p.

4.1.2 Wall pressure and skin-friction distributions

The distributions of pressure and skin friction along the pipe wall in many ways reflect the velocity field described above. Just downstream of the step, where there appears to be little direct influence of the free shear layer on conditions at the wall, the pressure is almost constant, decreasing only slightly with distance downstream (Fig. 5). A shallow minimum is reached about one third of the way to reattachment. In the reattachment region, where there is a direct interaction between the wall and the shear layer, the pressure rises gradually with distance downstream, C_p reaching about 0.25 at the reattachment point itself.

The distribution of mean skin friction coefficient C_f (Fig. 6 a), while qualitatively similar to that of C_p, more closely mirrors the local mean-velocity field. The minimum C_f, of -0.0007, is reached midway between separation and reattachment, the streamwise location where the mean backflow velocity reaches its maximum of $0.16\,U_{ref}$ (Fig. 3 a). The magnitudes of the mean skin friction coefficients in the recirculation region are large when based on the local backflow velocity (-0.03 at maximum). This fact, also noted by other workers studying this type of flow (Westphal et al. 1985, Castro and Haque 1987, for example), may indicate that laminar shear stress $\mu\partial U/\partial Y$ is important in the backflow. This possibility, and the structure of the backflow in general, is investigated and discussed in detail by Devenport and Sutton (1991).

The distribution of r.m.s. skin friction coefficient C'_f (Fig. 6 b), in many ways mirrors that of the peak turbulence intensity in the shear layer u'_p (Fig. 9 b). It rises with distance downstream from separation reaching a maximum at about 80% of the distance to reattachment, after which it gradually falls. As with u'_p this maximum disappears if the fluctuating skin friction is normalized on the edge-velocity of the shear layer, the rise continuing downstream beyond the limit of our measurements, at $X/H = 20.6$.

4.2 Effects of the centerbody

4.2.1 Velocity field

The primary effect of the centerbody, clearly visible in the streamlines (Fig. 4 a), it to deflect the flow towards the pipe

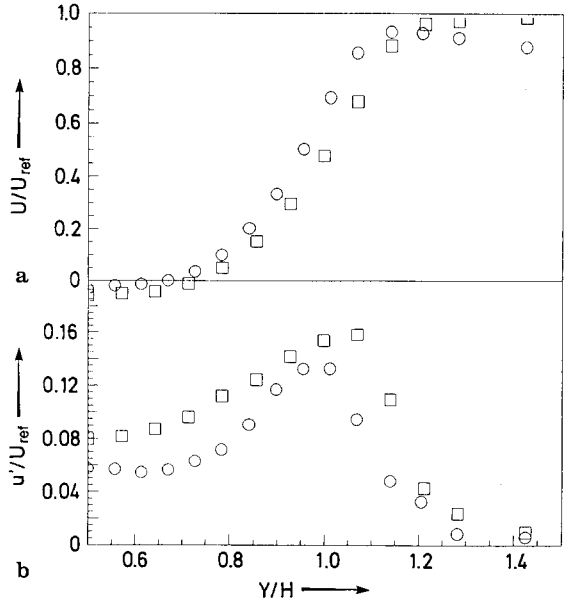

Fig. 10a and b. Comparison of shear layer velocity profiles in the datum flow ($X/H = 1.71$, squares) and in the flow with centerbody ($X/H = 1.57$, circles). **a** Mean velocity, **b** profiles of turbulence intensity

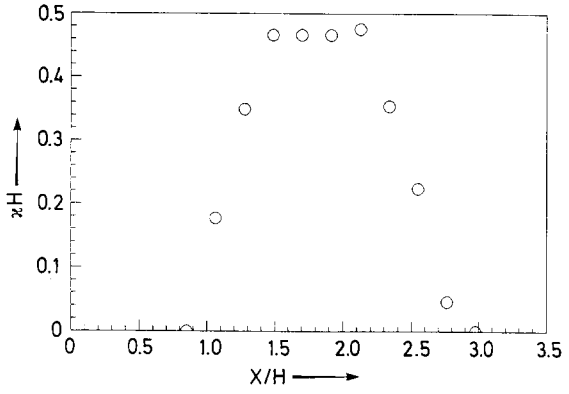

Fig. 11. Curvature of the dividing streamline in the flow with centerbody

wall causing early reattachment. The curvature of the dividing streamline is correspondingly increased, as is the angle at which it meets the wall (40° with the centerbody). The centerbody also accelerates the flow in the reattachment region creating a negative streamwise pressure gradient in the potential flow here. The mean velocity measurements suggest that the shear layer is much thinner in the reattachment region than in the datum flow (not surprising because of the shorter length over which it has grown). They also show that the peak backflow velocity ($-0.27\,U_{ref}$) is larger than in the datum flow and, relative to the reattachment position, occurs further downstream, at $X/X_r = 0.75$.

For a short distance downstream of separation the development of the turbulent shear layer is not greatly affected by the presence of the centerbody. This can be seen in Fig. 10 where mean-velocity and turbulence-intensity profiles measured at $X/H = 1.57$ with the centerbody and $X/H = 1.71$ in the datum flow are compared. The mean velocity profiles here are very similar. Turbulence intensities with the centerbody are, however, somewhat smaller, especially towards the low-speed side of the layer. The cause of this difference appears to be the strong shear layer curvature produced by the centerbody.

Castro and Bradshaw (1976) studied the effects of curvature on a mixing layer formed between a region of potential flow and one of still air. The layer, like the present flow, was curved towards its low speed side. The radius of curvature was never less than four times the mixing-layer thickness. They found that the mixing layer became thinner (i.e. its growth rate became negative) and the Reynolds stresses fell with distance along the layer in the region of maximum curvature. Downstream of the maximum, as the layer straightened out, the Reynolds stresses and growth rate rose again to levels above those normally encountered in uncurved mixing layers. Johnson and Hancock (1989) have observed similar effects.

The curvature of the shear layer in the flow with centerbody was estimated from the curvature of the dividing streamline. This streamline remains coincident with the locus of peak turbulence intensity over all but the last 10% its length (Fig. 4) and thus appears a more reliable marker of the shear layer center than in the datum flow. The curvature $\varkappa$ (inverse of radius of curvature), normalized with the step height H, is plotted as a function of X/H in Fig. 11. This figure shows the $\varkappa H$ reaching a maximum of about 0.46 between $X/H = 1.5$ and 2.1, corresponding to a radius of curvature that is about four times the shear-layer thickness here (judged from the mean-velocity profiles). It is therefore hardly surprising that turbulence intensities at $X/H = 1.57$ are lower than in the datum flow.

The effects of curvature can also be clearly seen in the variations of peak streamwise turbulence intensity and of vorticity thickness with X, included in Fig. 7. Note that with the centerbody these parameters could not be estimated from axial velocity measurements since, over a portion of its length, the shear layer was inclined at a significant angle to the axial direction. Instead these were estimated from corrected single hot-wire measurements of streamwise mean velocity and turbulence intensity. Furthermore, since these were measured in radial profiles, the maximum velocity gradient across the shear layer (required for the vorticity thickness) was estimated from the peak radial velocity gradient by dividing by $\cos\phi$, ϕ being the inclination of the dividing streamline to the X-axis.

Initially (for $X/H < 1.5$) both δ_ω and u'_p rise with distance downstream from separation. Because of the relatively wide spacing of points it is not possible to say with certainty whether this increase is the same as in the datum flow. However, such a conclusion would not be inconsistent with the data. After a short distance, though, shear layer curvature

starts becoming important and the rates of rise in δ_ω and u'_p decrease. Both parameters then reach maxima and begin to fall in the region of maximum curvature between $X/H = 1.5$ and 2.1. u'_p then behaves exactly as one would expect given Castro and Bradshaw's observations – reaching a minimum and then rising rapidly as the shear layer straightens out. u'_p then reaches a second maximum in the vicinity of reattachment.

Turbulence levels and the growth rate of the shear layer are, of course, also influenced by the presence of the recirculation zone. As in the datum flow we would expect turbulence levels in the shear layer to be increased by its re-entrainment of turbulent fluid. This may explain why the net reduction in u'_p due to curvature is somewhat smaller than might be expected given Castro and Bradshaw's results alone.

It is not possible, given the measurements presented here, to deduce the exact physics of the reattachment process. However, it is clear that as a consequence of the higher reattachment angle and thinner shear layer, this process occurs over a much shorter distance than in the datum flow. This is true instantaneously as well as on time average. Measurements presented by Devenport (1985) show that instantaneous flow direction changes at the wall associated with reattachment are all confined to a region between $X/X_r = 0.88$ and 1.16. (Instantaneous direction changes occur along the entire measured length of the datum flow.) In the region of sustained backflow immediately upstream of reattachment the turbulence intensity profiles (Fig. 4b, $X/H = 2.4$, 2.0) have peaks near $Y/H = 0.35$ that appear to be too close to the wall to be directly associated with the impinging shear layer and too far from it to be associated with the generation of turbulent energy by viscous stresses at the wall. This is possibly turbulence energy derived from the shear layer in the reattachment process (including three-dimensional developments) being convected upstream.

The flow structure downstream of reattachment initially changes very quickly. By $X/H = 5$ the mean-velocity gradient and peak in the turbulence intensity profile associated with the shear layer have almost completely dissipated. New boundary layers can be seen in Fig. 4 growing on the pipe wall and centerbody surface. This rapid development may be partly a consequence of the strong destabilizing curvature that this flow must experience as it is turned downstream in the reattachment region.

4.2.2 Wall pressure and skin friction distributions

With the centerbody, the region of approximately constant pressure immediately downstream of separation is much longer, relative to X_r, than without (Fig. 5). The minimum in C_p does not occur until $X/X_r = 0.75$ and is followed by a much more rapid rise than in the datum flow. Shortly downstream of reattachment C_p reaches a peak of about 0.28, after which it falls steeply as the flow accelerates into the gap between the centerbody and wall.

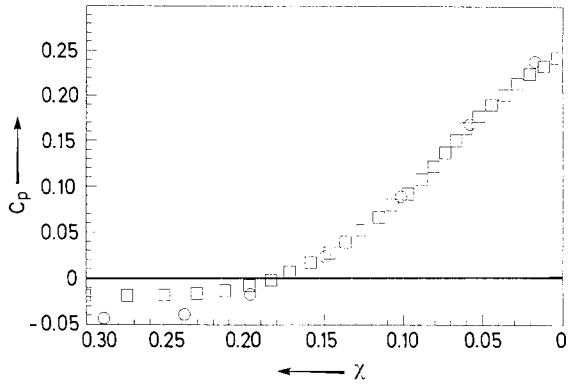

Fig. 12. Distributions of mean surface pressure coefficient along the test wall plotted in terms of the coordinate χ; squares, datum flow; circle, flow with centerbody

The minimum pressure coefficient is significantly lower than in the datum flow ($-.04$ compared to $-.02$) probably as a result of the higher backflow velocities in this case. Surprisingly, the pressure coefficient at reattachment (0.26) is almost the same. To this extent only, these measurements fit the correlation first proposed by Roshko and Lau (1965), that the pressure distribution should scale on the distance to reattachment. Otherwise, their difference in shape constitutes as extreme a departure from that correlation as has been reported. This departure can be accounted for qualitatively without reference to the details of the reattachment process. The distance over which most of the interaction of the reattaching shear layer with the wall takes place may be expected to vary like the length b in Fig. 1, the length over which extrapolations of the approaching shear layer intersect the wall. The ratio b/X_r will be reduced if the angle at which the shear layer approaches the wall is increased.

For the pressure distributions of the two present flows to be related the shear layer geometry must clearly be taken into account. One simple way of doing this is to plot the distributions in terms of a shear-layer centered coordinate χ, defined as $\chi \equiv n/s$, where "s" is distance along the shear layer centerline from separation and "n" distance normal to it, measured from the centerline to the wall (Fig. 1). If the dividing streamline is taken as the shear-layer centerline the pressure distributions of the datum flow and flow with centerbody agree well in the region of pressure rise when plotted against this coordinate (Fig. 12). Bearing in mind the sweeping assumptions it implies it is difficult to explain why this correlation exists. A clue comes from the fact that, when plotted in this way, the pressure distributions of other workers who have also published dividing streamline shapes (Moss and Baker 1980, Eaton and Johnson 1981) do not collapse to the curve of Fig. 12. It may be then that the correlation works for the flows because they only differ in geometry downstream of separation, and not in initial flow structure and conditions.

The effects of the centerbody on the mean skin-friction distribution (Fig. 6) are in many ways similar to its effects on

the pressure. The minimum in C_f is much lower with the centerbody (-0.003), presumably as a consequence of the higher backflow velocities, and occurs much closer to reattachment (at $X/X_r = 0.9$). The rise in C_f in the reattachment region is much more rapid, presumably because of the higher reattachment angle. This rapid rise, coupled with unsteadiness in the reattachment process, may explain the large maximum in fluctuating skin friction found here. Values of $C_{f\,\mathrm{r.m.s.}}$ in the vicinity of reattachment are as much as three times those in the datum flow.

5 Conclusions

Flow through an axisymmetric sudden expansion with and without a centerbody has been studied through velocity, pressure and skin friction measurements.

Without the centerbody a turbulent shear layer is formed by the separation of the flow at the expansion. Mean-velocity profiles in the shear layer are initially similar to those of an axisymmetric jet mixing layer. Turbulence levels are, however, higher and the growth rate of vorticity thickness lower. Reattachment of the shear layer appears to be a relatively gradual process. The dividing streamline meets the wall at a glancing angle of 17°. The locus of peak turbulence intensity never approaches the wall, moving only towards the centerline as it would in a free jet. The time mean distance to reattachment, 10.7 step heights, is long when compared that for most two-dimensional backstep flows. This may be because, relative to its surface area available for entrainment, the separated shear layer has to entrain a greater volume of recirculating fluid before reattaching in the axisymmetric than in the two-dimensional case. Normalized on separation conditions the peak turbulence intensity and r.m.s. skin-friction coefficient reach their maxima just upstream of the reattachment point. Normalized on local centerline velocity, however, these parameters continue to rise in the reattachment region.

Introducing the centerbody deflects the flow towards the pipe wall causing reattachment much earlier (at $X/H = 3.15$ on average). The curvature of the dividing streamline is correspondingly increased, as is the angle at which it meets the wall (40° with the centerbody). Initial development of the shear layer appears similar to that in the datum flow. Its greater curvature, however, soon becomes important in stabilizing its turbulence structure. Peak turbulence levels and vorticity thickness reach a maximum and then fall in the region of maximum curvature. Turbulence levels then rise again in the reattachment region. Relative to the distance to reattachment, the reattachment region is much shorter with the centerbody. This is because the shear layer is thinner and impinges at a higher angle. The rates of rise of wall static pressure and skin-friction coefficient C_p and C_f are much more rapid than in the datum flow and peak fluctuating skin-friction levels (found just downstream of reattachment) are 3 times greater. Distributions of C_p for the datum flow and flow with centerbody do not scale on the distance to reattachment. However, they collapse in the region of pressure rise when plotted in terms of a coordinate that takes into account shear layer geometry.

Acknowledgements

The authors are glad to acknowledge the financial support of the Royal Aircraft Establishment in performing this work. They would also like to thank Graham Evans and Borek Vokach-Brodsky for their contributions to the design and development of the apparatus.

References

Adams, E. W.; Johnston, J. P.; Eaton, J. K. 1984: Experiments on the structure of a turbulent reattaching flow. Dept. of Mech. Eng., Stanford University, Rept. MD-43

Baughn, J. W.; Hoffman, M. A.; Takahashi, R. K.; Launder, B. E. 1984: Local heat transfer downstream of an abrupt expansion in a circular channel with constant wall heat flux. J. Heat Transfer 106, 789–796

Bandyopadhyay, P. R. 1991: Instabilities and large structures in reattaching boundary layers. AIAA Journal 29, 1149–1155

Bradbury, L. J. S.; Castro, I. P. 1971: A pulsed-wire technique for velocity measurements in high turbulent flows. J. Fluid Mechanics 49, 657–691

Castro, I. P.; Bradshaw, P. 1976: The turbulence structure of a highly curved mixing layer. J. Fluid Mechanics 73, 265

Castro, I. P.; Dianat, M.; Bradbury, L. J. S. 1987: The pulsed-wire skin-friction measurement technique. Turbulent shear flows 5. Berlin Heidelberg New York: Springer, pp. 178–197

Castro, I. P.; Haque, A. 1987: The structure of a turbulent shear layer bounding a separation region. J. Fluid Mechanics 179, 439–468

Cherry, N. J.; Hillier, R.; Latour, M. E. M. P. 1984: Unsteady measurements in a separated and reattaching flow. J. Fluid Mechanics 144, 13

Devenport, W. J. 1985: Separation bubbles at high Reynolds number: measurement and computation, University of Cambridge, Ph.D. thesis. Also published as Report CUED/A-AERO/15, Cambridge University Engineering Department, 1989

Devenport, W. J.; Evans, G. P.; Sutton, E. P. 1990: A traversing pulsed-wire probe for velocity measurements near a wall. Exp. Fluids 8, 336–342

Devenport, W. J.; Sutton, E. P. 1991: Near-wall behavior of separated and reattaching flows. AIAA Journal 29, 25–31

Drewry, J. E. 1978: Fluid dynamic characterization of sudden expansion ramjet combustor flow fields. AIAA Journal 16, 313–319

Driver, D. M.; Seegmuller H. L. 1985: Features of a reattaching turbulent shear layer in divergent channel flow. AIAA Journal 23, 163–171

Durrett, R. P.; Stevenson, W. H; Thompson H. D. 1988: Radial and axial turbulent flow measurements with an LDV in an axisymmetric sudden expansion air flow. J. Fluids Engineering 110, 367–372

Eaton, J. K.; Johnston, J. P. 1980: Turbulent flow reattachment: an experimental study of the flow and structure behind a backward-facing step. Dept. Mech. Eng., Stanford University, Rept. MD-39

Freeman, A. R. 1975: Laser anemometer measurements in the recirculating region downstream of a sudden pipe expansion. Proceedings of the LDA Symposium, Copenhagen, pp. 704–709

Gould, R. D.; Stevenson, W. H.; Thompson H. D. 1990: Investigation of turbulent transport in an axisymmetric sudden expansion. AIAA Journal 28, 276–283

Gutmark, E.; Ho, C.-H. 1983: Preferred modes and the spreading rates of jets. Physics Fluids 26, 2932–2938

Ha Minh, H.; Chassaing, P. 1979: Perturbations of turbulent pipe flow. Turbulent Shear Flows 1, Berlin Heidelberg New York: Springer pp. 178–197

Johnson, A. E.; Hancock, P. E. 1989: The effect of extra strain rates of streamline curvature and divergence on mixing layers. 7th Symposium on Turbulent Shear Flows. Stanford University, CA, August 21–23, Chapters 28.5.1–28.5.6

Husain, Z. D.; Hussain, A. K. M. F. 1979: Axisymmetric mixing layer: influence of initial and boundary conditions. AIAA Journal 17, 48–54.

Hussain, A. K. M. F.; Husain, Z. D. 1980: Turbulence structure in the free mixing layer. AIAA Journal 18, 1462–1469

Kim, J.; Kline, S. J.; Johnston, J. P. 1978: Investigation of separation and reattachment of a turbulent shear layer: flow over a backward-facing step. Dept. Mech. Eng., Stanford University, Rept. MD-37.

Khezzar, L.; Whitelaw, J. H.; Yianneskis, M. 1985: An experimental study of round sudden expansion flows, 5th Symposium on Turbulent Shear Flows, Ithaca, N.Y., pp. 5.25–5.30

Kline, S. J.; McClintock, F. A. 1953: Describing uncertainties in single sample experiments. Mechanical Engineering 75, 3

Moon, L. F.; Rudinger, G. 1977: Velocity distribution in an abruptly expanding circular duct. J. Fluids Engineering 99, 226–230

Moss, W. D.; Baker, S. 1980: Recirculating flows associated with two-dimensional steps. Aeronautical Quarterly 31, 151

Pronchick, S. W.; Kline, S. J. 1983: An experimental investigation of the structure of a turbulent reattaching flow behind a backward-facing step. Dept. Mech. Eng., Stanford University, Rept. MD-42

Roshko, A.; Lau, J. C. 1965: Some observations on transition and reattachment of a free shear layer in incompressible flow. Proceedings of the Heat Transfer and Fluid Mechanics Institute 18, 157

Runchal, A. K. 1971: Mass transfer investigation in turbulent flow downstream of sudden enlargement of a circular pipe for very high Schmidt numbers. Int. J. Heat Mass Transfer 14, 781–792

Stevenson, W. H.; Thompson, H. D.; Craig, R. R. 1984: Laser velocimeter measurements in highly turbulent recirculating flows. J. Fluids Engineering 106, 173–180

Tutu, N. K.; Chevray, R. 1975: Crossed-wire anemometry in high intensity turbulence. J Fluid Mechanics 71, 785

Westphal, R. V.; Johnston, J. P.; Eaton, J. K. 1984: Experimental study of flow reattachment in a single-sided suddenly expansion. Dept. Mech. Eng., Stanford University, Rept. MD-41

Yang, B. T.; Yu, M. H. 1983: The flowfield in a suddenly enlarged combustion chamber. AIAA Journal 21, 92–97

Yavuzkurt, S. 1984: A guide to uncertainty analysis of hot-wire data. J. Fluids Engineering 106, 181